

Nucleation chronology and electronic properties of In(As,Sb,P) graded-composition quantum dots

Oliver Marquardt

Weierstraß-Institut für Angewandte Analysis und Stochastik, Leibniz-Institut im Forschungsverbund Berlin e.V.,
Mohrenstraße 39, 10117 Berlin, Germany
Email: oliver.marquardt@wias-berlin.de

Torsten Boeck

Institut für Kristallzüchtung, Leibniz-Institut im Forschungsverbund Berlin e.V.,
Max-Born-Straße 2, 12489 Berlin, Germany

Achim Trampert

Paul-Drude-Institut für Festkörperelektronik, Leibniz-Institut im Forschungsverbund Berlin e.V.,
Hausvogteiplatz 5–7, 10117 Berlin, Germany

Karen M. Gambaryan

Dept. of Physics of Semiconductors and Microelectronics, Yerevan State University,
1 A. Manoukian Str., Yerevan 0025, Armenia

Abstract—We have studied nucleation process and electronic properties of graded-composition quantum dots (GCQDs) grown from In-As-Sb-P in the liquid phase for application in mid-infrared devices like photoresistors or photoconductive cells. The GCQD ensemble exhibits diameters of 10 – 120 nm and heights of 2 – 20 nm. Compositional grading is a typical feature of quantum dots grown in liquid-phase epitaxy (LPE) and our GCQDs exhibit increasing Sb content to their top with a maximum Sb content of 20% and a decreasing P content with its maximum of approx. 15% at their bottom. We have performed systematic simulations of the electronic properties of the GCQDs using an eight-band $\mathbf{k} \cdot \mathbf{p}$ model taking strain and built-in electrostatic potentials into account. Here we have studied the influence of height and diameter of the GCQDs on their absorption spectra as close as possible to the systems observed in experiment. Combining data from the height and diameter distribution of the GCQDs ensemble with absorption energies of similar systems obtained from the simulations, we obtain an absorption spectrum of the ensemble. The simulated spectrum yields a maximum absorption at $3.829 \mu\text{m}$, which is extremely close to the one observed in experiment. Correspondingly, our simulation setup can be employed for a theory-guided design of GCQDs suited to the requirements of specific devices.

I. INTRODUCTION

Semiconductor quantum dots have attracted much research interest within the past years, due to their unique physical properties. They represent key building blocks of a number of novel optoelectronic applications ranging from single-photon sources, quantum computers, nanophotonic devices or photodetectors. For light absorption in the mid-infrared spectrum, the quaternary alloy $\text{InAs}_{1-x-y}\text{Sb}_x\text{P}_y$ plays a prominent role as both its absorption wavelength and lattice mismatch to a substrate can be controlled by the Sb and P contents x and y . Moreover, In(As,Sb,P)/InAs films, but also quantum dots, can be grown using the robust and simple liquid-phase epitaxy (LPE) technique [1]. A particular strength of the LPE is the

capability to produce nanostructures with intentional composition gradings [2], which facilitates significant improvements of the overall crystal quality thus of the optical properties.

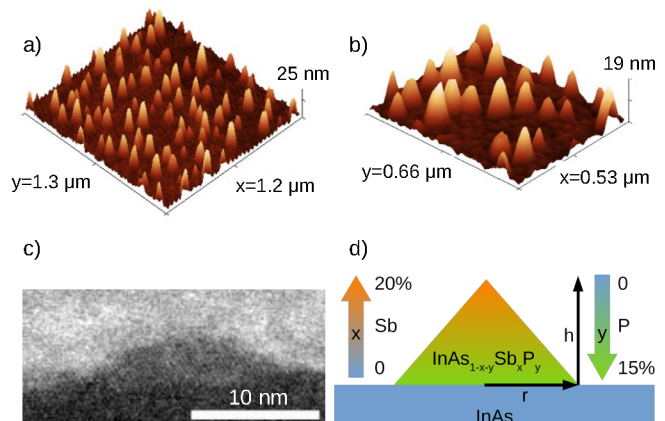


Fig. 1. a) and b) Oblique view AFM images of $\text{InAs}_{1-x-y}\text{Sb}_x\text{P}_y$ GCQDs grown on an InAs(100) substrate. c) cross-sectional bright-field STEM image of a GCQD. d) Schematic view of the model GCQD. The gradients of the Sb and P contents, x and y are indicated left and right of the schematic. The upper interface is to the vacuum [6].

II. IN(AS,SB,P) GRADED-COMPOSITION QUANTUM DOTS

In the following, we present a systematic study of the electronic properties of LPE-grown $\text{InAs}_{1-x-y}\text{Sb}_x\text{P}_y$ graded-composition quantum dots (GCQDs) for application in infrared photoresistors or photoconductive cells. Using continuum elasticity theory and an eight-band $\mathbf{k} \cdot \mathbf{p}$ model for zincblende crystals [3], implemented within the plane-wave framework of the SPHInX software library [4], [5], we compute elastic,

piezoelectric, and electronic properties of GCQDs as close as possible to those observed in experiment [6].

The GCQD ensemble was grown from In-As-Sb-P in the liquid phase with the composition x and y chosen to provide a compressive lattice mismatch of 2% to the InAs substrate at 540°C. Figure 1 a and b show oblique view atomic-force microscopy images of some of the GCQDs. Following scanning transmission electron microscopy analysis (cf. Fig. 1 c), we have assumed a flat, conical shape of our GCQDs with Sb (P) content increasing (decreasing) linearly towards the top and maximum values of $x = 0.20$ and $y = 0.15$ at the top (bottom) of the GCQDs.

III. SIMULATION OF THE ELECTRONIC PROPERTIES

The model GCQD for our simulations is depicted in Fig. 1 d. We have systematically varied diameter and height of the GCQDs, where the range of both parameters was taken from the GCQDs ensemble. All material parameters involved were taken from Ref. [7] In the first step, we have calculated the elastic properties of the GCQDs. Hydrostatic and Biaxial strains both have their extrema near the GCQDs tip, due to the Sb content x being largest in this area (cf. Fig. 2 a and b). The band diagram of a typical GCQD is shown in Fig. 2 c along its height. The system represents a type-II heterostructure with the conduction band minimum in the InAs substrate and the valence band maximum at the GCQDs tip. Furthermore, it can be seen that strain modifies the conduction band such that it becomes almost flat (the dashed line denotes the band diagram without influence of strain.). We note that built-in polarisation potentials resulting from strain are very small in our GCQDs.

As the electron is located in the InAs substrate, we have computed the charge density and energy of only the hole ground state in the next step. Figure 2 d shows the transition energy between hole ground state and InAs conduction band as a function of the GCQDs height h for different diameters d (indicated at the respective lines). The inset in Fig. 2 d shows a typical hole ground state charge density in a GCQD.

Finally, we have combined data from the diameter and height distribution of the GCQDs ensemble with the respective transition energies from our simulations (gray area in Fig. 2 d) to simulate an absorption spectrum for comparison with the absorption spectrum measured for our GCQDs ensemble (cf. Fig. 2 e). Absorption energies were corrected to room temperature using the Varshni relation [8]. The simulated spectrum fits the one observed extremely well with peak absorption wavelengths of 3.829 (simulation) and 3.83 μm (experiment).

IV. SUMMARY

We have performed a detailed analysis of nucleation process and electronic properties of In(As,Sb,P) QCQDs grown from the liquid phase. The electronic properties of the GCQDs were computed for model systems as close as possible to the experiment using an eight-band $\mathbf{k} \cdot \mathbf{p}$ model, taking strain and built-in electrostatic potentials into account. The absorption spectra obtained from our simulations are in a

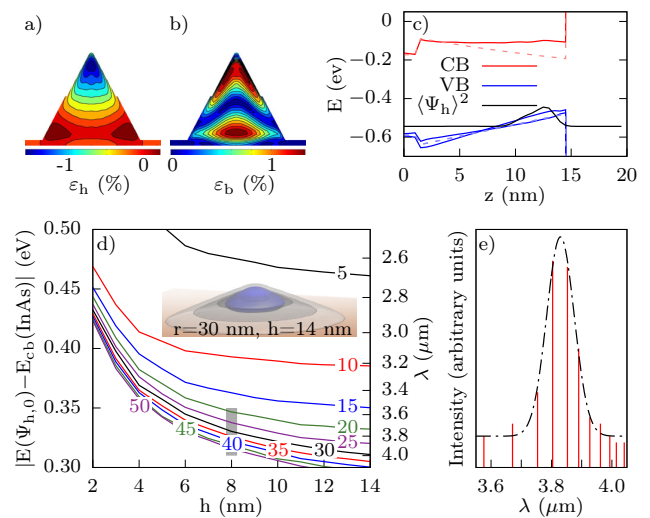


Fig. 2. a) and b) Hydrostatic and biaxial strain ϵ_h and ϵ_b of a model GCQD with $r = 30$ nm and $h = 14$ nm in a cross-section view (not to scale). c) Valence (blue) and conduction (red) bands along the central axis of the model GCQD. The dashed lines indicate the band behavior in the absence of strain. The respective hole ground state charge density is shown as a solid black line. d) Hole ground state energy (left axis) and corresponding wave length (right axis) with respect to the InAs conduction band edge as a function of height for different radii (given in nm at the respective lines) of the GCQDs at a temperature of 10°C. The inset shows the respective charge density (blue) of one selected system. The Sb content is indicated in white (0 – 5%), light (5–10%) and dark gray (10 – 15%) and black (15 – 20%) isosurfaces. e) Spectrum obtained from the diameter distribution of the GCQD ensemble and respective wave lengths obtained from our simulations for a GCQD height of 8 nm and radii from 20 to 50 nm (gray bar in d). A gaussian function has been fitted to the data and yields a maximum absorption at a wavelength of 3.829 μm with a FWHM of 120 nm (black dash-dotted line) [6].

very good agreement with those observed in experiment. We conclude that such simulations represent a valuable tool for a theory-guided design, suited to identify the most promising heterostructures for the demands of specific applications.

REFERENCES

- [1] Zh. I. Alverov, V. M. Andreyev, S. G. Konnikov, V. R. Larionov, and B. V. Pushny, *Kristall und Technik* **11**, 1013 (1976).
- [2] M. G. Mauk, A. N. Tata, and J. A. Cox, *J. Crystal Growth* **225**, 236 (2001).
- [3] T. B. Bahder, *Phys. Rev. B* **41**, 11992 (1990); Erratum: *Phys. Rev. B* **46**, 9913.
- [4] S. Boeck, C. Freysoldt, A. Dick, L. Ismer, and J. Neugebauer, *Comp. Phys. Commun.* **182**, 543 (2011).
- [5] O. Marquardt, S. Boeck, C. Freysoldt, T. Hickel, S. Schulz, J. Neugebauer, and E. P. O'Reilly, *Comp. Mat. Sci.* **95**, 280 (2014).
- [6] K. M. Gambaryan, T. Boeck, A. Trampert, and O. Marquardt, *Appl. Electron. Mat.* **2**, 646 (2020).
- [7] I. Vurgaftman, J. R. Meyer, and L. R. Ram-Mohan, *J. Appl. Phys.* **89**, 5815 (2001).
- [8] Y. P. Varshni, *Physica* **34**, 149 (1967).